Exact enumeration of self-avoiding walks on critical percolation clusters in 2–7 dimensions

2017 J. Phys. A: Math. Theor. 50 264002

(http://iopscience.iop.org/1751-8121/50/26/264002)

IOP Publishing Journal of Physics A: Mathematical and Theoretical

J. Phys. A: Math. Theor. **50** (2017) 264002 (17pp) https://doi.org/10.1088/1751-8121/aa6b91

Exact enumeration of self-avoiding walks on critical percolation clusters in 2–7 dimensions

Niklas Fricke and Wolfhard Janke

Institut für Theoretische Physik and Centre for Theoretical Sciences (NTZ), Universität Leipzig, Postfach 100920, D–04009 Leipzig, Germany

E-mail: niklas.fricke@itp.uni-leipzig.de and wolfhard.janke@itp.uni-leipzig.de

Received 4 November 2016, revised 24 March 2017
Accepted for publication 5 April 2017
Published 2 June 2017

Abstract

We study self-avoiding walks on critical percolation clusters by means of a recently developed exact enumeration method, which can handle walks of several thousand steps. We had previously presented results for the two- and three-dimensional cases; here we take a wider perspective and vary the system's dimensions up to $D = 7$, beyond the supposed upper critical dimension of $D_{\mathrm{uc}} = 6$. These results may serve to check analytical predictions and help understand how the medium's fractal structure impacts on the walks' scaling behavior.

Keywords: self-avoiding walks, percolation clusters, exact enumeration

(Some figures may appear in colour only in the online journal)

1. Introduction

Self-avoiding walks (SAWs) on critical percolation clusters are a simple model for polymers in highly disordered environments such as porous rocks or a biological cell [1, 2]. The system is also appealing from a theoretical perspective as it combines two of the most ubiquitous models from statistical physics. It has therefore been studied intensely in the past both analytically and numerically. However, despite its conceptual simplicity, the problem proved extremely challenging. Few reliable predictions exist for the SAWs' scaling exponents, and our qualitative understanding of the model is also still limited. In particular, it is unclear how the disorder and the medium's fractal structure, characterized by its various fractal dimensions, impacts the SAWs' asymptotic scaling behavior. This understanding is crucial when we want to generalize from the results and make predictions for real-world systems.

The main difficulty for numerical investigation of the problem can be overcome by making use of the self-similar geometry of critical percolation clusters to factorize the problem, in an

approach that we called scale-free enumeration (SFE) [3, 4]. In two preceding studies, we had used this method to investigate SAWs on critical percolation clusters in $2D$ [5] and $3D$ [6, 7]. Here we expand this perspective and look at systems in up to $7D$, above the supposed upper critical dimension of $D_{\mathrm{uc}} = 6$. The motivation for studying these high-dimensional systems is twofold. First, the results may contribute to a better understanding of how the fractal structure of a medium affects the SAWs' scaling behavior as the various fractal dimensions of critical percolation clusters depend in different ways on the embedding Euclidean dimension. Second, the results can be used to check analytical predictions, e.g. from Flory approximations [8, 9] and real-space [10, 11] or Fourier-space renormalization-group studies [12–16]. These latter rely on ϵ-expansions from the upper critical limit, so that they should be more accurate in higher dimensions. In particular, we want to verify whether $D = 6$ really is the upper critical dimension, where the scaling exponents take on mean-field values.

The remainder of the article is organized as follows. Section 2 gives a short overview of the topic, introducing the relevant concepts and summing up the state of research. In the following section 3, we specify our model and summarize the methods used to create the substrates (percolation clusters and cluster backbones) and to enumerate the SAWs. In section 4 we present our results concerning the scaling behavior of SAWs on critical percolation clusters. Finally, in section 5, we discuss our findings and compare them with analytical predictions.

2. Background and theory

The discrete self-avoiding walk is a fundamental model in polymer physics as it captures the asymptotic scaling behavior of flexible polymers in good solvent condition [17–20]. In particular, the increase of its mean squared end-to-end distance (or its squared radius of gyration) scales with the number of steps as

$$\left\langle R^2 \right\rangle \sim N^{2\nu}, \tag{1}$$

where ν is a universal scaling exponent. For regular lattices, the value of ν is approximated by the Flory formula,

$$\nu \approx \frac{3}{D+2} \quad (D < 4), \tag{2}$$

which stems from a mean-field calculation of the free energy. This approximation happens to be exact in $2D$, and its prediction in $3D$ is also astoundingly accurate ($\nu_{3D} = 0.587\,597(7)$ [21]). At the system's upper critical dimension of $D_{\mathrm{uc}} = 4$ the value becomes equal to the random walk exponent, $\nu_{\mathrm{RW}} = 1/2$.

The number of possible chain conformations Z increases according to a scaling law of the form

$$Z \sim \mu^N N^{\gamma-1}, \tag{3}$$

where μ is a lattice-dependent effective connectivity constant, and γ is another universal quantity, sometimes referred to as *enhancement exponent*.

This behavior is the same on any regular lattice, but what happens when disorder is introduced? Specifically, we consider a lattice with quenched random defects, i.e. sites where the walker cannot go. We then have to take two averages, one over all SAW conformations, $\langle \ldots \rangle$, and one over all realizations of the disorder, $[\ldots]$. *Quenched* randomness means that the conformational average for each individual disorder realization contributes uniformly to the total disorder average:

$$\left[\left\langle R^2\right\rangle\right] = \sum_{i=1}^{C} \left\langle R^2\right\rangle_i / C, \quad [Z] = \sum_{i=1}^{C} Z_i / C, \tag{4}$$

where C denotes the total number of disorder realizations in the considered ensemble. Here we consider the incipient cluster ensemble (IC), where each disorder realization consists of a lattice configuration with one SAW starting site that is randomly chosen on a percolating cluster (or cluster backbone) of non-defect sites.

The mean squared end-to-end distance for a system with quenched defects of a fixed concentration $1 - p$ also increases by a power law,

$$\left[\left\langle R^2\right\rangle\right] \sim N^{\nu_p}, \tag{5}$$

but there has been much controversy in the past regarding the question whether or when the exponent changes, i.e. when $\nu_p = \nu$ holds [10, 12, 22–25]. Here p refers to the concentration of non-defect sites (thus $\nu := \nu_1$). Eventually, the so-called Meir–Harris model [13] gained general acceptance, which predicts that the behavior is unchanged above the percolation threshold ($p > p_c$) but $\nu_{p_c} > \nu$. This is intuitive as the fractal dimension d_f of a critical percolation cluster is smaller than the Euclidean dimension, while it is the same above criticality. However, simply replacing D with the fractal dimension in the Flory formula (2) does not give reasonable estimates. A number of alternative Flory formulas have instead been derived based on mean-field arguments, which involve other properties of the critical clusters. These included the fractal dimension d_{BB} of the cluster backbone (the largest substructure that cannot be disjoined by removing a single site), the shortest-path dimension d_{min} and the walk dimension d_w, which characterizes the diffusivity on the cluster. (For an explanation of various properties of percolation clusters see, for instance, [26]. Estimates of the values from the literature are given in appendix A.) However, most of the proposed approximations could already be excluded based on numerical results [27]. The most prominent suggestion [9] links ν_{p_c} to various fractal exponents of the backbone,

$$\nu_{p_c} = \frac{2 + \alpha_{BB}}{d_{BB} + \alpha_{BB} d_{w,BB}}, \tag{6}$$

with

$$\alpha_{BB} = \frac{d_{min}}{d_{w,BB} - d_{min}}. \tag{7}$$

This approximation seems compatible with numerical results so far, but it has not yet been tested very thoroughly. More sophisticated analytical approaches estimate ν_{p_c} via perturbational field theory, making use of the relation between the SAW and the $O(n)$ model in the limit $n \to 0$ [28]. These should give exact predictions at the upper critical dimension (supposedly $D = 6$) and can be systematically ϵ-expanded to cover lower-dimensional systems. Unfortunately, however, the field-theory studies [14, 15] yielded conflicting results already for the second-loop term. This conflict could not yet be resolved numerically, as the most numerical tools could not handle sufficiently long SAWs in disorder.

There is even more uncertainty regarding the average number of chain conformations in quenched disorder. In the incipient cluster ensemble, it is not even certain whether the scaling law for $[Z](N)$ is still of the form of equation (3). The problem is that it is very difficult to estimate $[Z]$ numerically since the distribution of Z has extreme-value characteristics. It is considerably easier to consider the average entropy, $S = [\ln Z]$, or, equivalently, the *zeroth moment*, $Z_0 := \exp([\ln Z])$, since $\ln Z$ does not suffer from large deviations. Nonetheless, the

scaling behavior of $[\ln Z]$ has also been controversial [29–33]. Recently, we showed for the $3D$ case that $Z_0(N)$ does not follow a scaling law as equation (3) but seems to increase with a stretched exponential instead of the power-law factor [6].

3. Model and methods

We investigated SAWs on incipient percolation clusters for hypercubic lattices ($\mathbb{Z}^D$). On each cluster, we enumerated all SAW conformations of a given length N and measured their average end-to-end distances. This was done with the scale-free enumeration method described in detail in [4].

3.1. Creating the clusters

The percolation thresholds for $\mathbb{Z}^D$-lattices are not known exactly, but very accurate numerical estimates can be found in the literature. The specific values we used for p_c are given in appendix A, where we also compiled estimates for relevant fractal dimensions of the critical clusters from the literature. We also produced our own estimates for some fractal dimensions as a check for our settings.

We consider the ensemble of incipient clusters (IC average) and use the horizontal wrapping criterion to define percolation. This means a cluster percolates if it wraps around the lattice along one designated dimension ('horizontally'), assuming periodic boundary conditions. This choice has the advantage of yielding clusters that are translationally invariant (statistically) and suffer less finite-size effects compared to, e.g. when a lattice-spanning criterion is used [34].

Lattice sizes L were chosen depending on the planned number of SAW steps N. Ideally, one would like $L \geqslant 2N$, so that no SAW starting in the center can reach the edges[1]. Unfortunately, this is not practical in higher dimensions, where the lattices quickly become unwieldy. Instead, we used smaller lattices which were continued periodically, meaning that identical cluster areas can theoretically be reached via different boundaries. However, we chose $L(N)$ large enough so that this would only happen on a small fraction ($<10^{-3}$) of configurations to avoid introducing a significant bias. Note that the effect of this repetitiveness on the average end-to-end distances is very small since very few SAW conformations stretch that far. The actual sizes we used are given in appendix B.

The restriction to the incipient-cluster ensemble (also made in most preceding numerical studies) is convenient and probably reduces finite size-effects, but it also affects the fractal dimension in high dimensions: for $D \geqslant 7$ clusters that wrap the system have an increased fractal dimension of $d_\mathrm{f} = 2D/3$ rather than $d_\mathrm{f} = 4$ [35, 36]. However, we believe that this does not affect the SAWs, as the difference is only relevant on a very large scale.

To generate the clusters we used a recursive burning algorithm known as the Leath method [37]: initially, all sites are *unknown* except for one *occupied* seed site. In each frame of the routine, all *unknown* sites that are neighbors to *occupied* sites are set to *occupied* with probability p_c or marked as *defect*. This process is repeated until the routine runs out of *unknown* neighbors. If the resultant cluster percolates, it is used as substrate for the SAWs, otherwise it is discarded and the whole procedure is repeated until a percolating cluster is obtained. The easiest and fastest implementation of the burning algorithm uses a D-dimensional array to store the status of the sites, which we did for $D < 4$. In higher dimensions, however, this requires too much memory ($\sim L^D$), so instead we used a hash table storing only the *occupied* sites ($\sim L^{d_\mathrm{f}}$).

[1] Theoretically, increasing the lattice size further would still slightly change the medium's properties, but we found no measurable effect on the SAW statistics.

We also looked at SAWs on backbones of incipient percolation clusters, which have been suspected to be the only relevant part for determining the SAWs' asymptotic scaling behavior [8, 33, 38]. We defined the backbone of a percolating cluster as the path that wraps around the lattice plus all cluster sites that can be connected to that path via two distinct, non-intersecting routes. Several slightly different definitions have been used in preceding studies, but the practical differences are small and should not much affect the results for the SAWs. To extract the backbones, we used a variant of Tarjan's bridge-finding algorithm [39], which is easy to implement and quite efficient.

3.2. Scale-free enumeration (SFE)

Exact enumeration means that we look at all possible SAW conformations of a given length N, in contrast to Monte Carlo methods, where one tries to sample a representative subset. Since the number of chain conformations increases exponentially with N, exact enumeration will usually have exponential time complexity, seriously limiting the accessible lengths. In fact, only up to $N = 45$ steps on $2D$ clusters [40] and 40 steps on $3D$ clusters [33] have so far been handled by the straightforward 'brute-force' method. For regular lattices intricate enumeration methods have been developed to push the number of steps to $N = 71$ in $2D$ [41] and $N = 36$ in $3D$ [42, 43], but these cannot be easily translated to the case with disorder.

Fortunately though, the fractal structure of the critical clusters can be exploited to avoid exponential complexity by an appropriate factorization of the problem. The details of this approach are rather complicated, and for a comprehensive explanation and benchmarkings of the method we refer the interested reader to [4]. However, the main concepts are simple and shall briefly be outlined here.

The key observation is that critical percolation clusters are *finitely ramified fractals*, which means that they can be separated into disconnected pieces of similar size by removing only $O(1)$ sites [44]. The idea of SFE is to divide the cluster into such loosely connected regions ('cells') in order to factorize the enumeration procedure. Thanks to the self-similar nature of the system, this can be done on all length scales.

Concretely, the SFE method operates in the following way to obtain the number Z_N of conformations of N-step SAWs starting from a fixed site ('origin') and their mean squared end-to-end distance $\langle R^2 \rangle_N$:

(i) We reduce the size of the system by trimming the cluster to the sites that have a shortest-path (or chemical) distance of no more than N from the origin. This step is not strictly necessary, but it simplifies the problem and saves memory. In the following, we shall refer to this region as *root cell*.

(ii) We partition the cluster into a hierarchy of *cells* as shown in figure 1 for a miniature example. Cells are connected subsets of cluster sites. A cell may fully contain smaller cells (its *children*), but otherwise cells must be disjoint. This nesting of cells can be represented as a tree where the root cell is at the top[2] and contains the SAW origin. The method is only efficient if the partitioning meets the following criteria: first, all cells must contain few sites that lie outside of its children as this is where the SAW segments will be enumerated directly. Second, a cell must not have too many *links* to its *parent*, and the number of links to its children must also be small. This is because SAW segments must later be grouped depending on how they connect to parent and children, and the number of such groups can quickly get out of hand. To find a 'good' partitioning, we use a

[2] The idea of a tree with the root at the top is strange, but such is the standard terminology.

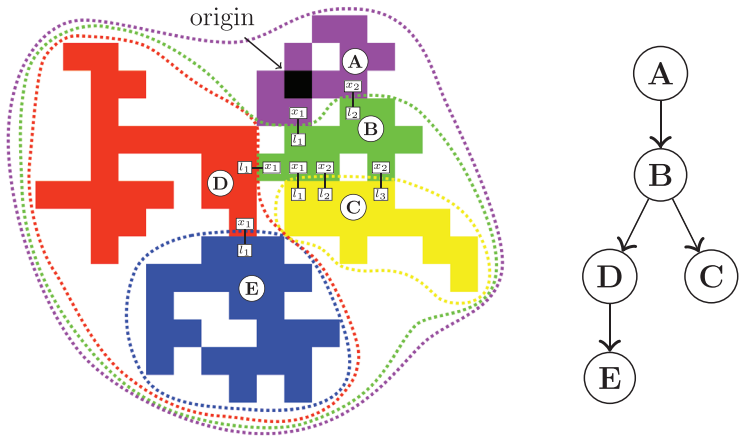

Figure 1. Partitioning of an exemplary cluster into a tree hierarchy of nested cells. The cluster has been cropped to $N = 15$ chemical shells around the origin (black site in cell A), the maximal SAW length considered in this example.

bottom-up strategy, where cells are repeatedly merged with their most strongly connected neighbors. Other clustering algorithms may work as well.

(iii) Next, we traverse the hierarchy in post-order to enumerate the SAW segments, i.e. we deal with each cell after all its children have been dealt with. Hence we start by enumerating the conformations $Z[n]$ of all SAW segments of length n within one of the smallest cells (without children), for which we use the standard enumeration method [25]. We group these segments according to where they link to the parent. Segments may terminate within a cell, in which case we also accumulate the distances to the origin $R^2_{\text{acc}}[n]$. For a cell with children, we additionally keep track of how segments pass through these. Apart from this, children are effectively treated as single sites with variable numbers of neighbors. Only after all segments through a cell have been enumerated are they 'connected' with the segments through the children. This is done via discrete convolution operations. In figure 1, e.g. the number $Z^D[n]$ of segments of length n within cell D is obtained as

$$Z^D[n] = Z^D_0[n] + \sum_{i=0}^{n} Z^D_1[i] Z^E[n-i], \tag{8}$$

where Z^D_1 and Z^D_0 are segments that do or do not connect to E, respectively, and Z^E are the segments within the child[3]. To obtain the corresponding accumulated squared distances R^2_{acc} we have to weight with the respective number of chains, e.g.

$$R^2_{\text{acc}}{}^{D}[n] = Z^D_0[n] R^2_{0,\text{acc}}{}^{D}[n] + \sum_{i=0}^{n} Z^D_1[i] Z^E[n-i] R^2_{\text{acc}}{}^{E}[n-i]. \tag{9}$$

Note, that the accumulated squared distances are equal to the mean times the respective number of conformations. These steps of enumeration and connecting the segments repeat up to the root, whose segments must link to the origin.

[3] Things get more complicated for multiple links and children, but the core concept is this.

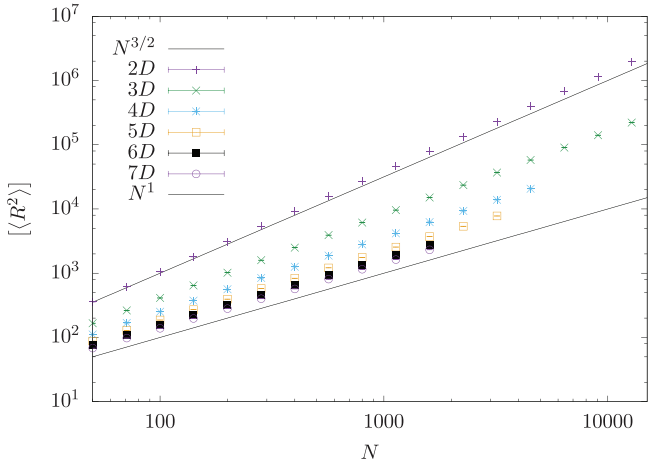

Figure 2. Results for the disorder average of the mean squared end-to-end distance as a function of the number of SAW steps on critical clusters in $D = 2 - 7$ plotted on a double-logarithmic scale. The lines correspond to the regular-lattice value in $2D$, $\nu_{1,2D} = 3/4$, and the mean-field value, $\nu_{\text{uc}} = 1/2$.

The procedure stops once the total number of segments within the root and their squared distances have been determined as these are our full SAWs. Note that the method performs a numerical real-space renormalization: we essentially integrate out the degrees of freedom of small cells, then decimate them in order to do the same for the next larger cells. If the partitioning is done well, the effort per cell for the actual 'brute-force' enumeration part thus remains constant on average, so that the total time complexity is polynomial rather than exponential. For our implementation, we measured a time increase of about $T \sim N^{2.4}$ [4]. Curiously, the exponent appears to be fairly constant in all dimensions though the amplitudes decrease very strongly with increasing D as the effective coordination number goes down. The reduced time complexity allows us to exactly enumerate SAWs of over $N = 10^4$ steps, easily amounting to 10^{2000} conformations. Note, however, that the method relies on the properties of the critical cluster; above p_c it only works to a fairly limited extent.

4. Results: SAW scaling behavior

4.1. Mean squared end-to-end distance

According to equation (5), the disorder average of the mean squared end-to-end distance increases with the number of steps as a power law, so that the exponent $2\nu_p$ results as the asymptotic slope when we plot $\left[\langle R^2 \rangle\right]$ versus N on a log-log scale. Such a plot is shown in figure 2 for systems of varying dimension, where we also plotted the slopes corresponding to the exactly known regular $2D$ case ($2\nu_{1,2D} = 3/2$) and to the regular upper critical limit ($2\nu_{\text{uc}} = 1$).

A detailed discussion of the results shall be presented in three slices. We start with the two most physically relevant cases, $D = 2$ and $D = 3$. These have also been studied most widely in the past. While the $3D$ results have already been published [6, 7], those for $2D$ are new and significantly more accurate than those from [5]. Next, we discuss the cases of $4D$ and $5D$. These have hardly been looked at before, but they are relevant for comparing with analytical results. Finally, we turn to the cases $6D$ and $7D$, i.e. at and beyond the supposed upper

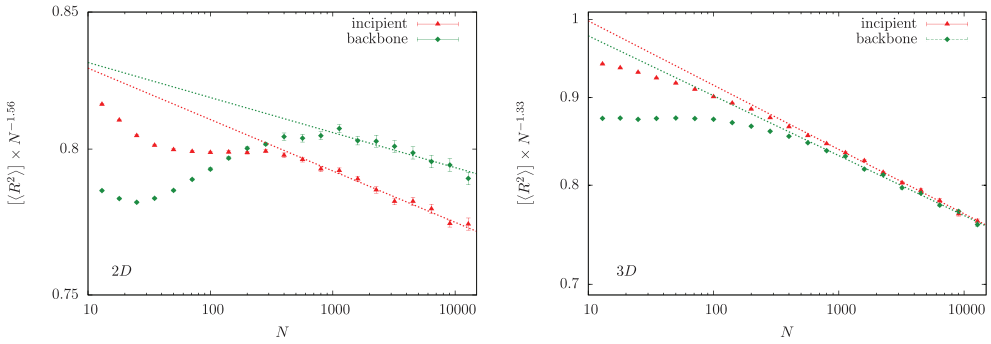

Figure 3. Scaled disorder averages of the mean squared end-to-end distance as a function of the number of SAW steps on critical clusters and cluster backbones in $2D$ (left) and $3D$ (right) on a double-logarithmic scale. The values have been divided by $\approx N^{2\nu_{pc}}$ for better visibility. Straight lines show least-squares power-law fits to the data in the range $N = 800$–$12\,800$ for $2D$ and $3D$ incipient clusters and $N = 1131$–$12\,800$ for $3D$ backbones.

critical dimension. These were included mainly to see whether an upper critical dimension of $D_{\mathrm{uc}} = 6$ can be verified numerically. For all cases, we considered walks on incipient clusters and backbones.

4.1.1. $D = 2$ and $D = 3$. We looked at two- and three-dimensional systems with walk lengths increasing in multiplicative steps of $\sqrt{2}$ from $N = 13$ up to $N = 12\,800$ ($=100 \times 2^7$). For each length we took independent samples of at least 5×10^4 randomly generated percolating clusters and backbones. The results for the mean squared end-to-end distance as a function of N and least-squares fits of equation (5) to the data are shown in figure 3 on a double-logarithmic scale. The y-axes have been rescaled by $\approx N^{2\nu_{pc}}$, so that the slopes are close to zero and more details are visible[4]. Note that while the conformational averages are evaluated exactly, we still have statistical fluctuations of the disorder averages reflected by the error bars. This noise, unfortunately, makes the use of powerful extrapolation techniques [19, 46, 47] that can be applied to exact enumeration data for regular lattices more difficult and less promising. Simple extrapolation techniques such as the method of successive slopes, see [33], did not appear to improve the quality of the results. More advanced methods such as Padé approximants might still somewhat improve the accuracy of the predictions even for noisy data [48], but this comes at the cost of simplicity and clarity, in particular as far as statistical error estimates are concerned, so that we decided to stick with the direct fitting approach.

As can be seen in figure 3, there are persistent finite-size corrections and the asymptotic scaling behavior seems to set in only after about $N = 1000$ steps in both cases. The effect in $2D$ is particularly interesting as the slope initially increases and later decreases again. These finite-size effects make clear why earlier numerical studies that were restricted to relatively short chains could not have revealed the true asymptotic behavior. We estimated the exponents simply by fitting equation (5) without correction terms. The ranges were chosen such that the reduced χ^2-values became close to one. To exemplify how we obtain our estimates, the $2D$ case shall be discussed in more detail. Table 1 shows the estimates from different ranges together with the reduced χ^2-values reflecting the quality of the fits. As the lower cut-off N_{min} for the fit range is increased, χ^2 decreases becoming close to one at around $N_{\mathrm{min}} = 400$

[4] The exponents we used are basically the estimates from [45]. As these were obtained from shorter SAWs on backbones, our backbone curves start out flat.

Table 1. Estimates of the exponent ν_{p_c} on critical $2D$ clusters and backbones for different lower cut-offs $N_{\min}$ of the fit ranges. The maximum was $N_{\max} = 12\,800$ in all cases. Also listed in the table are the effective number of degrees of freedom (dof) and the reduced χ^2-values. The line corresponding to our final estimates is highlighted.

$N_{\min}$	dof	ν_{IC}	${\chi^2}_{\mathrm{IC}}$	ν_{BB}	${\chi^2}_{\mathrm{BB}}$
13	19	0.776 81(5)	60.3	0.782 92(5)	72.3
50	15	0.777 63(8)	17.3	0.7828(1)	43.6
100	13	0.7770(1)	11.4	0.7811(2)	21.1
200	11	0.7761(2)	4.31	0.7796(2)	7.16
400	9	0.7753(3)	1.11	0.7777(4)	2.38
566	8	0.7751(3)	1.02	0.7773(4)	1.95
800	**7**	**0.7751(3)**	**1.14**	**0.7766(5)**	**1.05**
1600	5	0.7749(5)	1.02	0.7762(7)	0.39
3200	3	0.7756(9)	1.26	0.775(2)	0.15

(800 for backbones). The estimates also clearly seem to stabilize as all those with a lower cutoff above $N_{\min} = 400$ are consistent within the error bars. This clearly demonstrates that potential correction terms do not play a role at our present level of accuracy. For our final estimates we used the range $N = 800$–$12\,800$, where the fits for the incipient clusters and the backbones are both good. This range also worked best for the incipient clusters in $3D$, while $N_{\min} = 1131$ seemed best for the $3D$ backbones. As our final estimates we obtained:

$$2D: \quad \nu_{\mathrm{IC}} = 0.7751(3), \quad \nu_{\mathrm{BB}} = 0.7766(5), \tag{10}$$

$$3D: \quad \nu_{\mathrm{IC}} = 0.6462(4), \quad \nu_{\mathrm{BB}} = 0.6467(7). \tag{11}$$

In [6] we also tried to extend the fitting range by fitting the next confluent correction term for the $3D$ case. However, this did not convincingly improve the estimates, and in $2D$ capturing the inflection point would require at least two correction terms, introducing too many fit parameters.

The first thing to note about our results is that the estimates on incipient clusters and backbones are very close though the difference in $2D$ is not fully covered by the fit errors. However, the differences are marginal, so that the results can still be seen as supporting the hypothesis $\nu_{\mathrm{IC}} = \nu_{\mathrm{BB}}$ in our opinion. As already discussed [6], the $3D$ estimates are significantly smaller than those from earlier studies [33, 45, 49]. This is explained by the fact that the slope in figure 3 (right) is initially larger, especially for the backbones. The $2D$ result for ν_{IC} is consistent with that from [5] ($\nu_{\mathrm{IC}} = 0.7754(15)$) but significantly more accurate. Earlier $2D$ estimates [33, 45, 49] are not so far off either since the initial slopes ($N \leqslant 100$) in figure 3 (left) incidentally are very close to the asymptotic ones even though the behavior deviates in the intermediate regime.

4.1.2. 4D and 5D. In higher dimensions, we could not quite reach the same lengths as for $D = 2$ and 3. The limiting factor here was the time and memory needed to generate the clusters rather than the enumeration of the walks, which is actually significantly faster in higher dimensions. To reduce waste, we therefore considered several starting locations on each cluster (10 in $4D$ and 100 in $5D$). The (correlated) results thus obtained from one single cluster were then *binned* together, and we estimated the statistical errors from the fluctuations of the (uncorrelated) bin averages. We went up to $N = 4525$ and $N = 3200$ (increasing by multiplicative steps of $\sqrt{2}$) in $4D$ and $5D$, respectively, and took independent samples of at least 6×10^3

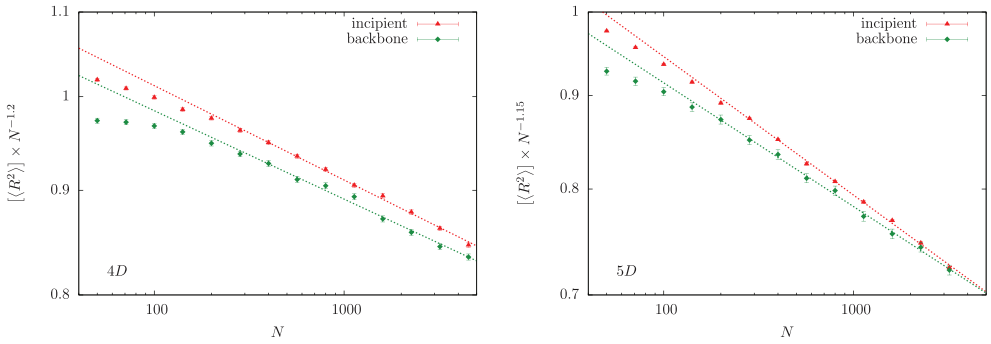

Figure 4. Scaled disorder average of mean squared end-to-end distance as a function of the number of SAW steps on critical clusters and cluster backbones in 4D (left) and 5D (right) on a double-logarithmic scale. The values have been divided by $\approx N^{2\nu_{pc}}$ for better visibility. Straight lines show least-squares power-law fits to the data ranges $N = 283$–4525 in 4D and $N = 283$–3200 in 5D, respectively.

and 1×10^3 clusters for each length. We here skipped the very small systems ($N \leqslant 50$), which had been included for $D \leqslant 3$ to facilitate comparison with earlier studies. The rescaled results for the mean squared end-to-end distances are shown in figure 4 together with least-squares fits of equation (5). As before, we chose the fit ranges by optimizing the reduced χ^2-values, which led to the estimates

$$4D: \quad \nu_{\mathrm{IC}} = 0.5769(5), \quad \nu_{\mathrm{BB}} = 0.5784(7), \tag{12}$$

$$5D: \quad \nu_{\mathrm{IC}} = 0.5371(4), \quad \nu_{\mathrm{BB}} = 0.5411(13). \tag{13}$$

As in 2D and 3D, our estimates in 4D are significantly smaller than one from a previous numerical study of shorter SAWs on (backbones of) critical percolation clusters ($\nu_{\mathrm{BB},4D} = 0.591(6)$ [49]) in accordance with the initially larger slopes in figure 4 (left). We are not aware of any previous numerical estimates for the 5D case.

The exponents from incipient clusters and backbones are again quite close. In 5D, ν_{BB} is somewhat larger, but since the fits in that case are not particularly good (especially for the backbones), the results can still be reconciled with the hypothesis $\nu_{\mathrm{IC}} = \nu_{\mathrm{BB}}$. Note that the error bars are significantly larger on the backbone data points. This is because the backbones are much less massive than the full clusters, so that the correlations caused by using multiple starting points are stronger.

4.1.3. 6D and 7D. The upper critical dimension for the system is supposed to be the same as for percolation, namely $D_{\mathrm{uc}} = 6$. This makes sense if we assume that the SAWs' scaling behavior is somehow determined by the fractal structure of the medium, and all fractal dimensions take on mean-field values at D_{uc}. However, directly at D_{uc} one also expects persistent logarithmic corrections [50–52]. Since these are notoriously difficult to fit, we also looked at the 7D case. In both 6D and 7D, we went up to $N = 1600$ steps and took samples of 1×10^3 clusters for each length with 100 randomly chosen starting locations per cluster. The results for the mean squared end-to-end distances can be seen in figure 5. Also shown in the figure are the best fits of equation (5), from which we obtained our final estimates

$$6D: \quad \nu_{\mathrm{IC}} = 0.5153(4), \quad \nu_{\mathrm{BB}} = 0.521(2), \tag{14}$$

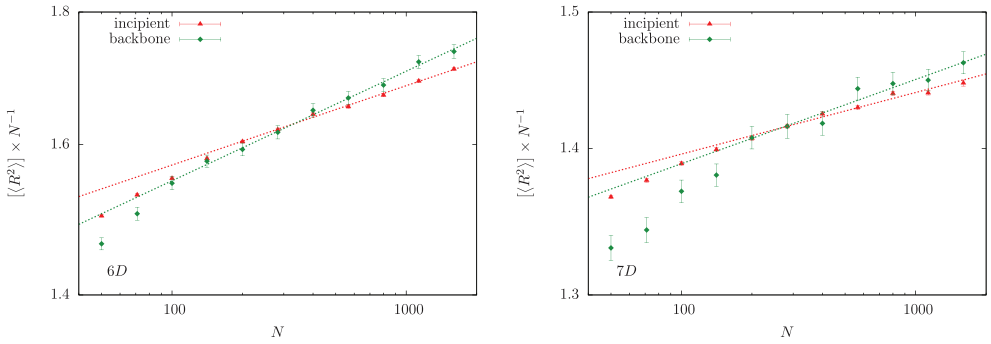

Figure 5. Scaled disorder average of the mean squared end-to-end distance as a function of the number of SAW steps on critical clusters in $6D$ (left) and $7D$ (right) and cluster backbones on a double-logarithmic scale. The values have been divided by N for better visibility. Straight lines show least-squares power-law fits to the data in the range $N \geqslant 200$.

$$7D: \quad \nu_{\mathrm{IC}} = 0.5068(4), \quad \nu_{\mathrm{BB}} = 0.509(2). \tag{15}$$

In $7D$, the exponents are reasonably close to the random walk exponent of 1/2, but in $6D$ they are significantly larger. As mentioned, this may partly be blamed on logarithmic correction terms (although the fits without corrections do not seem too bad). The results from backbones and incipient clusters are again quite similar. It should be pointed out that the data for these high-dimensional cases is less reliable since the affordable system sizes were much smaller ($N = 1600$ is still rather long, but the extensions of the lattices L are very limited; see appendix B). The fact that the estimates for ν_{p_c} resulted substantially larger than 1/2 in $6D$ does therefore not disprove that the upper critical dimension is 6, but neither is it a resounding numerical confirmation.

4.2. Average entropy $[\ln Z]$

It is very difficult to estimate the average number of chain conformations $[Z]$ from a random sample of disorder conformations (incipient clusters or backbones). Since the possibilities multiply at each step, each Z_i can be thought of the result of a multiplicative random process and the distribution hence resembles a log-normal. This means that the average is determined by rare events and much larger than the typical value. In $2D$, for instance, the maximum value of Z from our sample of 5×10^4 incipient clusters was over 70 orders of magnitude larger than the median and larger than the sum of all the rest. However, it is probably still far below the true average, which will practically always be underestimated by the mean over any finite sample. While this bias increases with N, the problem already clearly manifests itself for $N = 60$ [53] and may affect the estimates even earlier. Rather than sampling $[Z]$ directly, it is therefore more promising to gauge the distribution of $\ln Z$, which allows to calculate $[Z]$ approximately. In [6] we did this for the $3D$ case by simply assuming $\ln Z$ to be normally distributed. This seemed reasonable since the distribution indeed closely resembled a Gaussian, but it still introduced an uncontrolled systematic error, prohibiting any definite conclusions regarding the asymptotic scaling behavior of $[Z]$.

Here we simply avoid the problem of large deviations by focusing on the average entropy, $S = [\ln Z]$, and the zeroth moment, $Z_0 = \exp(S)$. These are easier to access numerically, but their asymptotic scaling behavior has been a controversial topic as well, and as many as five

Table 2. Results obtained by fitting equation (17) to the average entropy per step $[\ln Z]$ for SAWs on critical percolation clusters (top) and backbones (bottom) in different dimensions. For $D \geqslant 4$, the amplitude was fixed to $a = 1$.

Incipient clusters						
D	fit range	χ^2	a	μ_0	b	ζ
2	800–12 800	1.64	1.2(1.1)	1.4464(6)	0.6(4)	0.47(7)
3	800–12 800	0.52	0.7(6)	1.3119(5)	1.3(5)	0.48(5)
4	283–4525	0.77	1 (fixed)	1.2145(2)	2.12(8)	0.496(7)
5	283–3200	4.21	1	1.1551(2)	3.35(9)	0.514(6)
6	200–1600	0.85	1	1.1189(3)	5.4(2)	0.553(7)
7	200–1600	0.63	1	1.0960(2)	7.9(2)	0.589(6)
Backbones						
D	fit range	χ^2	a	μ_0	b	ζ
2	800–12 800	0.67	0.9(1.0)	1.4468(5)	1.1(5)	0.51(6)
3	800–12 800	1.18	0.8(7)	1.3121(4)	1.8(5)	0.51(4)
4	283–4525	0.55	1 (fixed)	1.2141(3)	2.2(2)	0.51(2)
5	283–3200	0.67	1	1.1561(6)	4.3(8)	0.62(4)
6	200–1600	2.84	1	1.1198(7)	7(2)	0.71(5)
7	200–1600	0.09	1	1.0957(7)	5(2)	0.67(6)

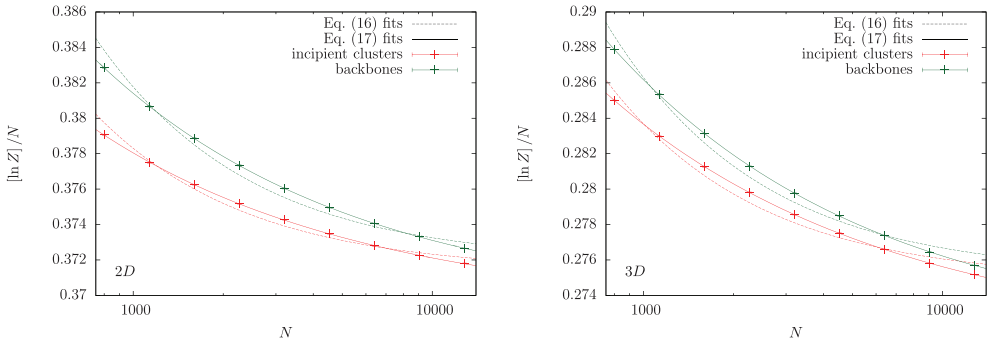

Figure 6. Average entropy per step for SAWs on incipient percolation clusters (red) and their backbones (green) in 2D (left) and 3D (right) plotted on a log-linear scale. The curves correspond to fits of equations (16) (dashed) and (17) (solid).

different scaling laws have been proposed. Perhaps the most obvious idea is that $Z_0(N)$ should follow a scaling law as equation (3) [33, 54], so that

$$[\ln Z]\,/N \sim \ln \mu_0 + (\gamma_0 - 1)\ln N/N + \ln a/N. \tag{16}$$

However, this is clearly refuted by our data. Indeed, as can be seen in figure 6 for the $2D$ and $3D$ cases, the behavior is much better captured by a scaling law of the form

$$[\ln Z]\,/N \sim (\ln \mu_0)(1 + bN^{-\zeta}) + \ln a/N. \tag{17}$$

The results for the fit parameters are given in table 2. For $D \geqslant 4$, our data is also clearly inconsistent with equation (16). However the amount of data here was insufficient to fit all

Table 3. Our numerical estimates for ν_{p_c} on incipient clusters and backbones in different dimensions (second and third column). Also listed are Flory approximations from equations (6) and (7) as well as the field-theory results ν_{p_c}(RG1) [14] and ν_{p_c}(RG2) [15, 16].

D	ν_{IC}	ν_{BB}	ν_{p_c}(Flory)	ν_{p_c}(RG1)	ν_{p_c}(RG2)
2	0.7751(3)	0.7766(5)	0.7592(7)	0.7853 . . .	0.7414 . . .
3	0.6462(4)	0.6467(7)	0.644(5)	0.6783 . . .	0.6537 . . .
4	0.5769(5)	0.5784(7)	0.584(4)	0.5951 . . .	0.5842 . . .
5	0.5371(4)	0.5411(13)	0.535(3)	0.5357 . . .	0.5329 . . .
6	0.5153(4)	0.521(2)	0.5	0.5	0.5
7	0.5068(4)	0.509(2)	0.5	0.5	0.5

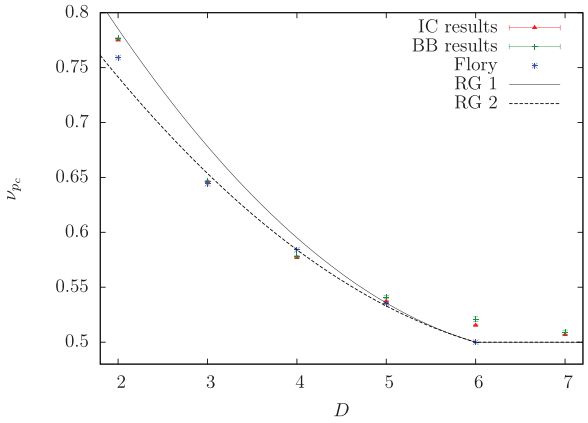

Figure 7. Results for ν_{p_c} on incipient clusters (red) and backbones (green) for different dimensions juxtaposed with analytical predictions. The blue asterisks correspond to Flory estimates from equations (6) and (7). The lines represent the field-theory estimates from [14] (solid) and [15] (dashed).

parameters in equation (17), so we had to fix the amplitude a to one. This seems permissible since $a \approx 1$ in $D = 2, 3$ and its overall effect is quite small anyway.

5. Summary and discussion

We have used the novel scale-free enumeration method to investigate self-avoiding walks on critical percolation clusters on hypercubic lattices in dimensions $D = 2$–7. In table 3 we present an overview of our estimates for the exponents characterizing the asymptotic scaling behavior of the mean squared end-to-end distances for SAWs on incipient critical percolation clusters and their backbones. Also listed are analytical predictions from the most promising Flory approximation, equation (6), where we plugged in the values from appendix A, and field-theoretical studies. A plot of these values is shown in figure 7. Overall, the agreement is best with the Flory approximation. Among the predictions from field theory, the curve from [15, 16] fits better to our results. Only in $2D$ is the prediction from [14] closer, but this is where the results of the ϵ-expansions are least reliable anyhow. Note that these predictions are obtained by directly evaluating the second-order ϵ-expansions from [14] and [15] at

$\epsilon = 6 - D$. As discussed in [55], it might be more accurate to consider the respective [1]/[2] Padé approximants. However, this gives larger results which fit our data less well.

Our study showed the importance of being able to study large system sizes for such multifractal models as finite-size corrections are very persistent. The asymptotic behavior seems to set in earlier on higher-dimensional clusters, where an SAW is less likely to interact with itself across a large number of steps. In all dimensions, the results for ν_{p_c} from incipient clusters and backbones are very close, though not always consistent within the fit errors. Still, at least in lower dimensions, where the data are most reliable the agreement is convincing. On balance, the findings hence support the 'backbone hypothesis', $\nu_{\mathrm{IC}} = \nu_{\mathrm{BB}}$. However, the results on the backbones are consistently 'worse' in the sense that the asymptotic behavior sets in later, so that studying the backbones instead of the full clusters is generally not a more efficient way to access the asymptotic scaling exponent as assumed in some previous works.

Finally, we presented empirical evidence for a scaling law for the average entropy $S = [\ln Z]$ per monomer involving a power-law term $N^{-\zeta}$ with ζ around 0.5 in all dimensions. This translates to an unusual stretched exponential behavior for the zeroth moment of the number of chains. As we argued in [6] this would imply a similar behavior for the number of chains $[Z]$ if the distribution of $\ln Z$ were close enough to a Gaussian so that the approximation of calculating $[Z]$ from its mean and variance is valid, i.e. $[Z] \sim \mathrm{e}^{S+\sigma^2_{\ln Z}/2}$. However, this issue still requires closer investigation.

Acknowledgments

The article is dedicated to Prof. Tony Guttmann on the occasion of his 70th birthday. The work was funded by the Deutsche Forschungsgemeinschaft (DFG) via FOR 877 (project P9) under Grant No. JA 483/29-1 and Sonderforschungsbereich/Transregio SFB/TRR 102 (project B04). We are grateful for further support from Graduate School GSC 185 'BuildMoNa,' Deutsch-Französische Hochschule (DFH) through the Doctoral College '$\mathbb{L}^4$' under Grant No. CDFA-02-07, and an Institute Partnership Grant with Lviv, Ukraine, by the Alexander von Humboldt Foundation (AvH) under Grant No. 3.4–Fokoop–DEU/1117877.

Appendix A. Properties of critical percolation clusters

The percolation thresholds for hypercubic lattices have been determined very precisely in previous studies; see table A1. By contrast, some fractal exponents have not yet been measured very accurately, so that we could obtain more accurate results by analyzing the clusters used in this study. We estimated d_{f} and d_{BB}, respectively, by fitting the average mass of the incipient cluster and the backbone against the lattice extension L; d_{min} was obtained by fitting the average chemical distance between two sites on a cluster versus L. The results were on the whole in excellent agreement with previous findings; for instance we estimated $d_{\mathrm{f},3D} = 2.5230(2)$ in perfect agreement with [56]. Table A2 shows the (to our knowledge) most accurate values available. Our own estimates are marked with an asterisk. Note that in $7D$, the values of d_{f}, d_{min} and d_{BB} change to $2D/3 = 14/3$, $D/3$, and $D/3$, respectively, for incipient clusters in systems with periodic boundary conditions [35, 36], which was confirmed by our numerical findings: $d_{\mathrm{f}} = 4.65(1)$, $d_{\mathrm{min}} = 2.331(9)$ and $d_{\mathrm{BB}} = 2.32(2)$. The walk dimension for the backbone was calculated via the relation (see [1])

$$d_{\mathrm{w,BB}} - d_{\mathrm{BB}} = d_{\mathrm{w}} - d_{\mathrm{f}}. \tag{A.1}$$

Table A1. Values for the percolation thresholds on hypercubic lattices used in this work.

D	p_c
2	0.592 746 21(13) [34]
3	0.311 607 68(15) [57]
4	0.196 8861(14) [58]
5	0.140 7966(15) [58]
6	0.109 017(2) [58]
7	0.088 9511(9) [58]

Table A2. Estimates for various fractal dimensions of critical percolation clusters and their backbones. Values marked with an asterisk are estimates obtained in this work.

D	2	3	4	5	$\geqslant 6$
d_f	91/48 [59]	2.522 95(12) [56]	3.044(2) *	3.517(7) *	4
d_{min}	1.130 77(2) [60]	1.3756(3) [56]	1.604(3) *	1.813(3) *	2
d_w	2.8784(8) [61]	3.88(3) [1]	4.68(8) [62]	5.50(6) [62]	6
d_{BB}	1.6434(1) [57]	1.8736(5) *	1.932(8) *	1.93(16) [63]	2
$d_{w,BB}$	2.6260(9)	3.23(3)	3.57(8)	3.9(2)	4

Appendix B. Choice of lattice extensions

The lattice extensions L were adjusted to avoid that SAWs could 'feel' the boundaries, while trying not to waste too much time and memory (in higher dimensions). The precise values that we used are listed in table B1.

Table B1. Numbers of SAW steps N and lattice extensions L used for different dimensions.

N	$2D$	$3D$	$4D$	$5D$	$6D$	$7D$
50	100	52	33	25	20	14
71	142	67	41	31	24	17
100	200	86	51	37	28	20
141	282	111	64	45	34	24
200	400	143	80	54	41	29
283	566	184	100	66	48	35
400	800	237	125	79	58	41
566	1132	305	156	96	69	49
800	1600	392	195	117	83	59
1131	2262	504	243	141	99	70
1600	3200	649	303	170	119	84
2263	4526	836	379	206		
3200	6400	1076	473	252		
4525	9050	1384	590			
6400	12 800	1782				
9051	18 102	2293				
12 800	25 600	2951				

References

[1] Ben-Avraham D and Havlin S 2000 *Diffusion and Reactions in Fractals and Disordered Systems* (Cambridge: Cambridge University Press)
[2] Chakrabarti B K (ed) 2005 *Statistics of Linear Polymers in Disordered Media* (Amsterdam: Elsevier)
[3] Fricke N and Janke W 2013 *Eur. Phys. J. Spec. Top.* **216** 175–9
[4] Fricke N and Janke W 2016 *Leipzig preprint*
[5] Fricke N and Janke W 2012 *Europhys. Lett.* **99** 56005
[6] Fricke N and Janke W 2014 *Phys. Rev. Lett.* **113** 255701
[7] Fricke N and Janke W 2015 *Phys. Rev. Lett.* **115** 149902 (erratum)
[8] Rammal R, Toulouse G and Vannimenus J 1984 *J. Phys.* **45** 389–94
[9] Aharony A and Harris A B 1989 *J. Stat. Phys.* **54** 1091–7
[10] Le Doussal P and Machta J 1991 *J. Stat. Phys.* **64** 541–78
[11] Hovi J and Aharony A 1997 *J. Stat. Phys.* **86** 1163–78
[12] Kim Y 1983 *J. Phys. C: Solid State Phys.* **16** 1345–52
[13] Meir Y and Harris B 1989 *Phys. Rev. Lett.* **63** 2819–22
[14] Von Ferber C, Blavatska V, Folk R and Holovatch Y 2004 *Phys. Rev.* E **70** 035104
[15] Janssen H K and Stenull O 2007 *Phys. Rev.* E **75** 020801
[16] Janssen H K and Stenull O 2012 *Phys. Rev.* E **85** 051126
[17] Flory P J 1969 *Statistical Mechanics of Chain Molecules* (New York: Interscience)
[18] de Gennes P G 1976 *Scaling Concepts in Polymer Physics* (Ithaca, NY: Cornell University Press)
[19] Guttmann A J 1987 *J. Phys. A: Math. Gen.* **20** 1839–54
[20] Vanderzande C 1998 *Lattice Models in Polymer Physics* (Cambridge: Cambridge University Press)
[21] Clisby N 2010 *Phys. Rev. Lett.* **104** 055702
[22] Chakrabarti B K and Kertész J 1981 *Z. Phys.* B **44** 221–3
[23] Kremer K 1981 *Z. Phys.* B **45** 149–52
[24] Harris A B 1983 *Z. Phys.* B **49** 347–9
[25] Lam P M 1990 *J. Phys. A: Math. Gen.* **23** L831–6
[26] Stauffer D and Aharony A 1992 *Introduction to Percolation Theory* (London: Taylor and Francis)
[27] Kim Y 1992 *Phys. Rev.* A **45** 6103–6
[28] de Gennes P 1972 *Phys. Lett.* A **38** 339–40
[29] Derrida B 1984 *Phys. Rep.* **103** 29–39
[30] Machta J and Kirkpatrick T R 1990 *Phys. Rev.* A **41** 5345–56
[31] Vanderzande C and Komoda A 1992 *Phys. Rev.* A **45** R5335–8
[32] Grassberger P 1993 *J. Phys. A: Math. Gen.* **26** 1023–36
[33] Ordemann A, Porto M, Roman H E, Havlin S and Bunde A 2000 *Phys. Rev. E* **61** 6858–65
[34] Newman M E J and Ziff R M 2001 *Phys. Rev.* E **64** 016706
[35] Aizenman M 1997 *Nucl. Phys.* B **485** 551–82
[36] Heydenreich M and van der Hofstad R 2011 *Probab. Theory Relat.* **149** 397–415
[37] Leath P L 1976 *Phys. Rev.* B **14** 5046–55
[38] Blavatska V and Janke W 2009 *Phys. Rev.* E **80** 051805
[39] Tarjan R E 1974 *Inf. Process. Lett.* **2** 160–1
[40] Singh A R, Giri D and Kumar S 2009 *Phys. Rev.* E **79** 051801
[41] Jensen I 2004 *J. Phys. A: Math. Gen.* **37** 5503–24
[42] Schram R D, Barkema G T and Bisseling R H 2011 *J. Stat. Mech.* P06019
[43] Schram R D, Barkema G T and Bisseling R H 2013 *Comput. Phys. Commun.* **184** 891–8
[44] Coniglio A 1982 *J. Phys. A: Math. Gen.* **15** 3829–44
[45] Blavatska V and Janke W 2008 *Europhys. Lett.* **82** 66006
[46] Gaunt D S and Guttmann A J 1974 Asymptotic analysis of coefficients *Phase Transitions and Critical Phenomena* (*Series Expansions for Lattice Models*) vol 3 ed C Domb and M S Green (New York: Academic) pp 181–243
[47] Guttmann A J 1989 Asymptotic analysis of power-series expansions *Phase Transitions and Critical Phenomena* vol 13, ed C Domb and J L Lebowitz (New York: Academic) pp 1–234
[48] Dekeyser R, Iglói F, Mallezie F and Seno F 1990 *Phys. Rev.* A **42** 1923–30
[49] Blavatska V and Janke W 2008 *Phys. Rev. Lett.* **101** 125701

[50] Wegner F J 1976 The critical state, general aspects *Phase Transitions and Critical Phenomena* vol 6, ed C Domb and M S Green (New York: Academic) pp 7–124
[51] Kenna R, Johnston D A and Janke W 2006 *Phys. Rev. Lett.* **96** 115701
[52] Kenna R, Johnston D A and Janke W 2006 *Phys. Rev. Lett.* **97** 155702
[53] Fricke N and Janke W 2012 *Phys. Proc.* **34** 39–43
[54] Roman H E, Porto M, Ordemann A, Bunde A and Havlin S 1998 *Phil. Mag.* B **77** 1357–71
[55] Blavatska V and Janke W 2010 *Phys. Proc.* **3** 1431–5
[56] Wang J, Zhou Z, Zhang W, Garoni T M and Deng Y 2013 *Phys. Rev.* E **87** 052107
[57] Xu X, Wang J, Zhou Z, Garoni T M and Deng Y 2014 *Phys. Rev.* E **89** 012120
[58] Grassberger P 2003 *Phys. Rev.* E **67** 036101
[59] Nienhuis B 1984 *J. Stat. Phys.* **34** 731–61
[60] Zhou Z, Yang J, Deng Y and Ziff R M 2012 *Phys. Rev.* E **86** 061101
[61] Grassberger P 1999 *Physica* A **262** 251–63
[62] Adler J, Meir Y, Aharony A, Harris A and Klein L 1990 *J. Stat. Phys.* **58** 511–38
[63] Hong D C and Stanley H E 1983 *J. Phys. A: Math. Gen.* **16** L475–81